ISSN 1063-7834, Physics of the Solid State, 2007, Vol. 49, No. 10, pp. 1923–1931. © Pleiades Publishing, Ltd., 2007.
Original Russian Text © V.P. Kravchuk, D.D. Sheka, 2007, published in Fizika Tverdogo Tela, 2007, Vol. 49, No. 10, pp. 1834–1841.

MAGNETISM AND FERROELECTRICITY

Thin Ferromagnetic Nanodisk in Transverse Magnetic Field

V. P. Kravchuk and D. D. Sheka

Kiev Taras Shevchenko National University, Kiev, 03127 Ukraine
e-mail: Waldemar@univ.kiev.ua

Received November 29, 2006; in final form, February 15, 2007

Abstract—The magnetization of a ferromagnetic nanodisk is studied using micromagnetic modeling. It is demonstrated that, under an external magnetic field applied perpendicular to the disk surface, magnetic phase transitions can occur between uniform states, between uniform and vortex states, and between vortex states with different directions of polarization. A simple variation model is proposed describing the observed magnetic states quantitatively.

PACS numbers: 75.75.+a, 75.40.Mg, 75.30.Kz, 75.10.Hk

DOI: 10.1134/S1063783407100186

1. INTRODUCTION

One of the most prominent advancements in the field of magnetism in recent years has been the use of nanotechnology for preparation and study of magnetic nanoscale structures [1, 2]. The distribution of magnetization in nanoparticles depends substantially on the particle size, geometry, and material parameters and can be nonuniform if the particle size exceeds the typical single-domain particle size. For soft magnetic materials, the single-domain particle size is of the order of the exchange length $l = \sqrt{A/4\pi M_S^2}$, where A is the exchange constant and M_S is the saturation magnetization. In particular, in a nanoparticle shaped like a cylinder (nanodisk), the uniform state is unstable with respect to the vortex formation if the disk diameter is larger than (3–4)l [3].

Magnetic nanoparticles are a subject of interest in nonlinear physics. Investigations of nonlinear excitations in nanoparticles and control of their properties with, e.g., a magnetic field go beyond purely scientific curiosity. A nanodisk in a vortex state is a promising candidate for storing a bit of information in high-density magnetic storage devices and fast magnetic memory and for use in very sensitive sensors [4]. The state representing a bit is usually associated with the direction of magnetization of the vortex core (vortex polarization). It is well known that vortices in easy-plane magnets can switch polarization under the influence of a magnetic field applied along the normal to the disk plane; as the strength of the transverse field is increased, the vortices that are polarized against the field lose stability [5, 6]. The switching effect was studied numerically by the Monte Carlo method in [7]. However, this conclusion was reached ignoring the magnetic-dipole interaction, which significantly affects the phenomena. At the same time, the switching of the vortex polarization was observed experimentally in [8] in permalloy disks wherein the vortex state is stabilized by the magnetic-dipole interaction. The micromagnetic modeling of the switching effect performed in [9] for relatively thick disks indicates that the possible switching mechanism is the formation of a Bloch point in the center of the vortex. The typical size of Bloch points is $d_{\mathrm{BP}} \sim 20$ nm [9]. However, in nanodisks with thicknesses of less then d_{BP}, this mechanism of vortex polarization switching is no longer advantageous. In this paper, we demonstrate that the switching of a thin disk is accompanied by the formation of an in-plane vortex.

The purpose of this paper is to investigate the behavior of a nanodisk in an external field applied along the disk axis. The paper is organized as follows. In Section 2, we consider magnetization switching in a disk uniformly magnetized in the disk plane (the planar state). As the field increases, an anhysteretic transition occurs to a state uniformly magnetized along the disk axis (z state).

If the size of the disk is sufficiently close to the single-domain particle size but is less than it, then the magnetization switching of a uniformly magnetized particle can proceed via an intermediate vortex state (Subsection 3.1). As the particle size is increased further, the ground state of the particle becomes vortical. The transition from the vortex state to the uniform z state takes place at substantially higher fields than does the transition from the uniform planar state to the uniform z state (Subsection 3.2). The former transition is characterized by hysteresis, which is due to an additional transition associated with the switching of the vortex polarization. This effect is discussed in Section 4.

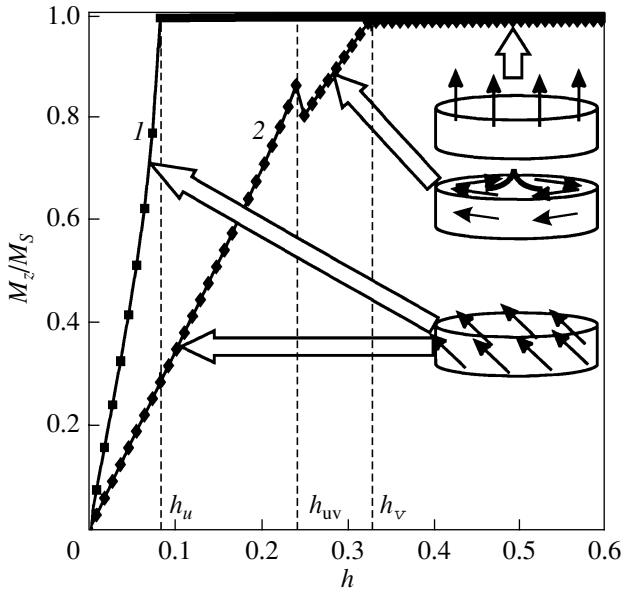

Fig. 1. Field dependence of the magnetization along the external field for disks whose ground state is uniformly magnetized in the disk plane. The data are obtained by micromagnetic modeling for 20-nm-thick permalloy disks (*1*) 30 and (*2*) 50 nm in diameter.

2. UNIFORM MAGNETIC STATE OF A NANODISK

Let us consider a thin disk with an aspect ratio $\varepsilon = d/2R$, where d is the thickness of the disk and R is its radius. We describe the distribution of spins in the disk in a continuum model using the normalized magnetization $\mathbf{m} = \mathbf{M}/M_S$ and the standard angular parameterization $\mathbf{m} = \{\sin\theta\cos\varphi, \sin\theta\sin\varphi, \cos\theta\}$. In the absence of a magnetic field, the energy of the uniformly magnetized disk is determined solely by the interaction of the surface magnetostatic charges. In the disk uniformly magnetized along the x axis, the energy (normalized by $\pi R^2 d M_S^2$) is determined by the demagnetization factor N_x [10]:

$$\mathcal{E}^u = 2\pi N_x, \quad N_x = \frac{2}{3\pi\varepsilon}\left[\frac{\varepsilon^2}{m}K(m) + \frac{1-\varepsilon^2}{m}E(m) - 1\right].$$

Here, $m = 1/\sqrt{1+\varepsilon^2}$; and $K(x)$ and $E(x)$ are complete elliptic integrals of the first and second kind, respectively.

Let an external magnetic field be applied perpendicular to the disk plane. We assume that the magnetization remains uniform and turns toward the field so that the angle between them is θ_u. The normalized magnetic energy of this state is given by

$$\mathcal{E}^u = 2\pi(N_z\cos^2\theta_u + N_x\sin^2\theta_u - 2h\cos\theta_u), \quad (1)$$

where $h = H/4\pi M_S$ is the normalized magnitude of the applied field H. For an axially symmetric particle, the demagnetization factor is $N_z = 1 - 2N_x$. Minimizing energy (1) with respect to θ_u, we get

$$\cos\theta_u = \frac{h}{h_u}, \quad \mathcal{E}^u = 2\pi\left(N_x - \frac{h^2}{h_u}\right), \quad h_u = N_z - N_x. \quad (2)$$

The quantity h_u describes the saturation field under which the uniform state with susceptibility $\chi_u = 1/4\pi h_u$ turns into a uniform saturated state with a magnetization directed along the z axis. This transition is described by curve *1* in Fig. 1, showing the results of computer simulation using the OOMMF program package for three-dimensional micromagnetic modeling [11].

The modeling is performed using the following material parameter values of permalloy $Ni_{80}F_{20}$: $A = 2.6\times10^{-6}$ erg/cm (in SI, $A^{SI} = 2.6\times10^{-11}$ J/m) and $M_S = 8.6\times10^2$ G ($M_S^{SI} = 8.6\times10^5$ A/m); the anisotropy of permalloy is disregarded. These parameter values correspond to an exchange length $l = \sqrt{A/4\pi M_S^2} \approx 5.3$ nm ($l^{SI} = \sqrt{A/\mu_0 M_S^2}$). The saturation field value $h_u \approx 0.08$ obtained by the modeling is in agreement with a theoretical estimate $h_u \approx 0.11$.For an infinitely thin disk, we have $h_u = 1$, which corresponds to the field of a uniformly magnetized plane in the z state. In general, $h_u < 1$. The dependence of h_u on the disk thickness is shown in Fig. 2 by the dashed line.

3. NANODISK IN A VORTEX STATE

Until now, we assumed that the system is in a uniform state. This is true only for particles of a sufficiently small size. As the dimensions of a particle are increased, its magnetization is distorted and a vortex state becomes energetically favorable. For a vortex distribution $\theta = \theta(r)$ and $\varphi = \chi \pm \pi/2$ (where r and χ are polar coordinates in the disk plane), the normalized exchange energy is given by

$$\mathcal{E}^v_{ex} = \frac{4\pi l^2}{R^2}\int_0^R\left[\theta'^2 + \frac{\sin^2\theta}{r^2}\right]rdr.$$

The magnetostatic energy of the vortex distribution is determined by surface charges $\sigma(\mathbf{r}) = \cos\theta(\mathbf{r})$,

$$\mathcal{E}^v_{MS} = \frac{1}{2\pi R^2 d}\int_S dS\int_{S'} dS'\frac{\sigma(\mathbf{r})\sigma(\mathbf{r}')}{|\mathbf{r}-\mathbf{r}'|}. \quad (3)$$

The function $\theta(r)$ minimizes the total energy functional and is, in general, a solution to an integrodifferential equation [12], which can only be analyzed approximately. The problem is significantly simplified for thin disks. In the absence of a magnetic field, the vortex has a bell-shaped profile and can be very accurately described using the following ansatz [13] (see also [14,

p. 265]): $\cos\theta = \exp(-r^2/W^2)$. Here, the typical size of the vortex core W is a variational parameter. For infinitely thin particles, the nonlocal magnetostatic energy (3) reduces to the effective anisotropy energy [15–17].

In the presence of a magnetic field, the ground state of the system is changed and the approach described above has to be modified. We use the following ansatz [18]:

$$\cos\theta(r) = f(r/W)(\mu - \cos\theta_v) + \cos\theta_v. \qquad (4)$$

Here, $\mu = \cos\theta(0)$ is the magnetization at the center of the vortex and $\cos\theta_v$ is the equilibrium magnetization far from the vortex. Note that, in general, θ_v does not coincide with θ_u in Eq. (2) obtained for the uniform case. We will describe the structure of the vortex core $f(x)$ using a Gaussian distribution $f(x) = \exp(-x^2)$, which is in good agreement with the results of simulation [19]. The total energy of a thin disk in a vortex state, including the Zeeman interaction energy with a magnetic field, can be written as

$$\frac{\mathscr{E}^v}{2\pi} = \frac{2l^2}{R^2}\int_0^{R/W} xdx\left\{\frac{\eta^2 f'(x)^2}{\sin^2\theta_v + \eta f(x)[2\cos\theta_v + \eta f(x)]} + \frac{\sin^2\theta_v + \eta f(x)[2\cos\theta_v + \eta f(x)]}{x^2}\right\} + N_z\cos^2\theta_v - 2h\cos\theta_v + \frac{2\eta^2\mathscr{C}_1 W^2}{R^2} + \frac{4\eta\mathscr{C}_2 W^2}{R^2}(\cos\theta_v - h), \qquad (5)$$

$$\mathscr{C}_1 = \int_0^{R/W} f^2(x)xdx, \quad \mathscr{C}_2 = \int_0^{R/W} f(x)xdx,$$

$$\eta = \mu - \cos\theta_v.$$

In order to calculate the nanodisk energy, it is necessary to minimize the total energy (5) with respect to the equilibrium magnetization θ_v and the size of the vortex core W. In general, this problem can be solved only numerically. Note that, in the absence of a field, the problem can be solved analytically [19]. In this case, $\theta_v^0 = \pi/2$ and $W^0 \approx l\sqrt{2}$.

3.1. Transition from the Uniform State to a Vortex State

Let us consider a disk in a uniform state. As the magnetic field is increased, the nanodisk energy decreases following a square law $\Delta\mathscr{E}^u \sim -h^2$, in accordance with Eq. (2). However, the structure of the vortex state changes insignificantly in small fields; therefore, its interaction with the field follows a linear law $\Delta\mathscr{E}^u \sim -h$ (see Eq. (5)). It is naturally to assume that a transition from the uniform state to a vortex state will occur at a certain critical field h_{uv}. Detailed calculations show that this transition does not take place in extremely thin disks; the energy of the vortex state is always larger than that of the uniform state (Fig. 3a). The variation of the magnetization with the field in this case is described by curve *1* in Fig. 1. However, this transition becomes possible as the disk thickness increases (Fig. 3b). In this case, the magnetization of a disk changes discontinuously at a characteristic field h_{uv} (curve *2* in Fig. 1).

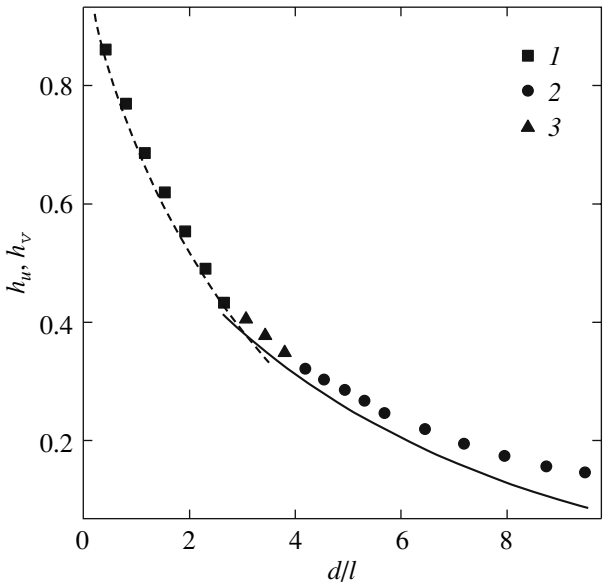

Fig. 2. Saturation field as a function of the disk thickness. The dashed line corresponds to the saturation field of the uniform state h_u given by Eq. (2), and the solid line is the saturation field related to the vortex state h_v in Eq. (9). Points are data from micromagnetic modeling for (*1*, *2*) disks whose ground states are uniform planar and vortex states, respectively, and (*3*) disks having a uniform planar ground state and passing through an intermediate vortex state during magnetization switching. Modeling is performed for permalloy disks 26 nm in radius.

By performing a numerical analysis of the energies of the uniform and vortex states described by Eqs. (2) and (5), respectively, we constructed the ground-state diagram for the disk (Fig. 4). Solid lines *1*, *2*, and *3* in the diagram are defined by the equations

$$\mathscr{E}^v\big|_{h=0} = 2\pi N_x,$$
$$\mathscr{E}^v\big|_{h=0} = 2\pi N_z, \qquad (6)$$
$$N_x = N_z,$$

respectively. This phase diagram is in good agreement with the calculations performed in [20, 21], and with the results of micromagnetic modeling obtained in [19, 22].

Using the criterion

$$(\mathscr{E}^v - \mathscr{E}^u)\big|_{h=0}(\mathscr{E}^v - \mathscr{E}^u)\big|_{h=h_u} < 0, \qquad (7)$$

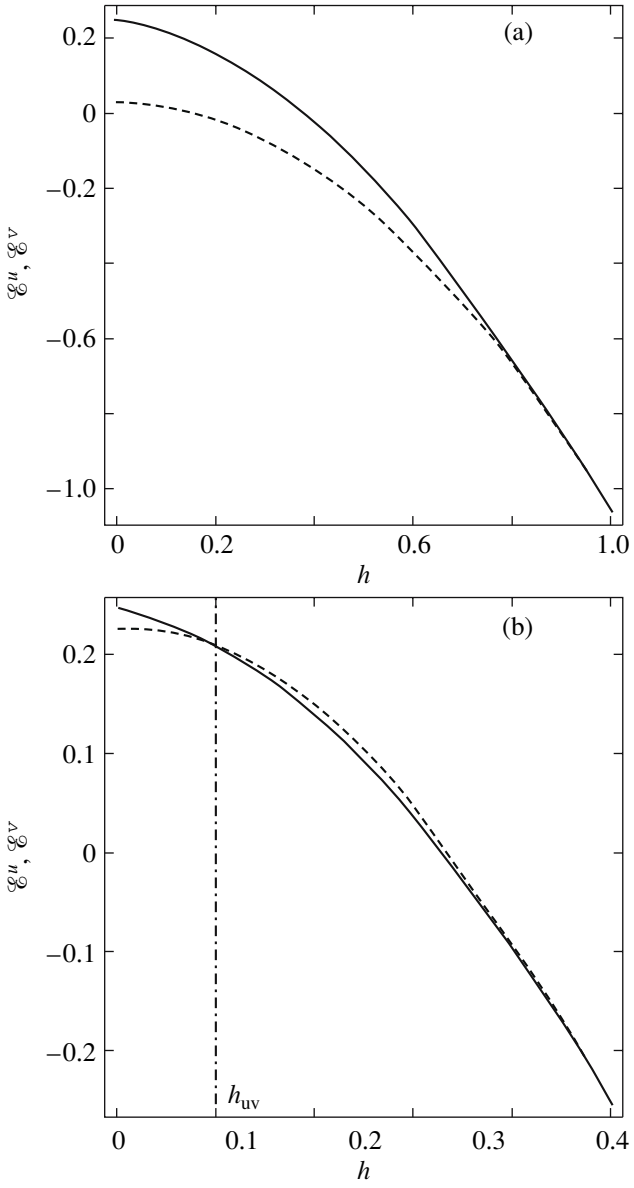

Fig. 3. Energy of a nanodisk as a function of external magnetic field calculated using Eqs. (2) and (5) for permalloy disks 27 nm in radius. The dashed lines correspond to a single-domain state, and the solid lines correspond to a vortex state. The disk thickness d is (a) 1 and (b) 20 nm.

we also found the ranges of geometric parameter values of the disk over which transitions from the uniform planar state to a vortex state occur under a magnetic field (hatched region in Fig. 4). By solving the equation $\mathcal{E}^u = \mathcal{E}^v$ numerically with allowance for condition (7), one can find the critical field for the transition from the uniform to vortex state. A calculation performed for the disk parameter values indicated in Fig. 1 (curve *2*) gives $h_{uv} \approx 0.19$, which is close to the result of modeling $h_{uv} \approx 0.24$.

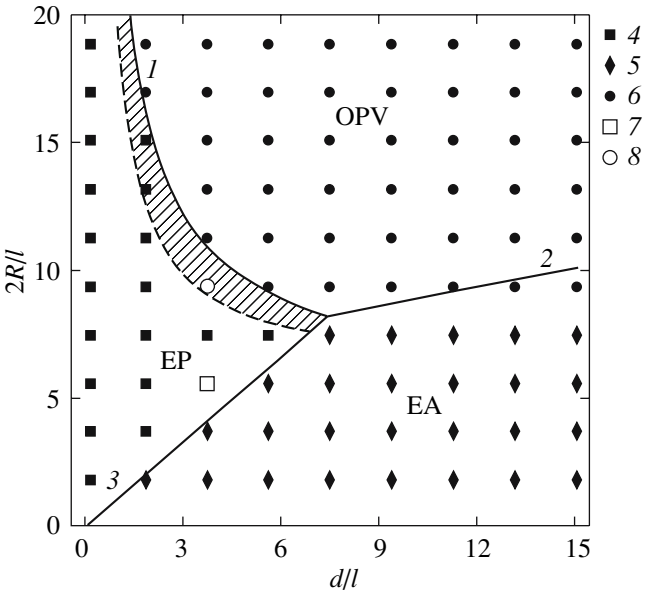

Fig. 4. Ground-state diagram of disks in the absence of a magnetic field. OPV is the vortex state, EP is the uniform planar state, and EA is the uniform z state (with a magnetization perpendicular to the disk plane). The hatched region corresponds to the disks that pass through an intermediate vortex state during the remagnetization process. Curves *1–3* are theoretical calculations based on Eq. (6), and points *4–6* show the disk sizes for which, according to micromagnetic modeling, the ground states are EP, EA, and OPV, respectively. Points *7* and *8* indicate disk sizes for which the magnetization behavior in an external field is shown in Fig. 1.

3.2. Transition from the Vortex State to a Uniform State

Now, we consider the transition from the vortex state to a uniform z state characterized by a saturation field h_v. Note that, in the absence of a field, the disk can be either in the uniform or vortex state.

Upon the transition to the saturated state, we have $\cos\theta_v \approx 1$. Therefore, we can expand energy (5) in a power series in $\cos\theta_v$ around the above value:

$$\frac{\mathcal{E}^v}{2\pi} \simeq N_z - 2h_v + 2[N_z - N_v - h_v - \mathcal{C}(1-h_v)](\cos\theta_v - 1) + \ldots,$$

$$N_v = \frac{l^2}{R^2}\int_0^{R/W}\left\{\frac{2[1-f(x)]}{x^2} + \frac{f'^2(x)}{2[1-f(x)]}\right\}xdx, \quad (8)$$

$$\mathcal{C} = 2\frac{W^2}{R^2}\int_0^{R/W} f(x)xdx.$$

In the case where the trial function $f(x) = \exp(-x^2)$ is used, for sufficiently large radius values $R \gg W$, we

arrive to the following asymptotic estimates:

$$N_v \approx 2\frac{l^2}{R^2}\ln\frac{R}{W}, \quad \mathscr{C} \approx \frac{W^2}{R^2}.$$

Minimizing energy (8) with respect to $\cos\theta_v$ and W, we get

$$h_v = \frac{N_z - N_v - \mathscr{C}}{1 - \mathscr{C}}, \quad W = \frac{l}{\sqrt{1 - h_v}}. \qquad (9)$$

Thus, the size of the vortex core at which the transition to the saturated state occurs is determined by the disk dimensions R and d and the exchange length l in the following way:

$$W = R\omega(x), \quad x = 1 + [1 - N_z]R^2/l^2, \qquad (10)$$

where the function $\omega(x)$ is implicitly defined by the relation $2\ln\omega + \omega^{-2} = x$, where $0 < \omega < 1$ and $x > 1$. An analysis shows that, as $R \longrightarrow \infty$, the size of the vortex core W tends to infinity, but $W/R \longrightarrow 0$.

In the other limiting case $R \ll W \longrightarrow \infty$, according to Eq. (8), we have $N_v \longrightarrow 0$ and $\mathscr{C} \longrightarrow 1$ and Eq. (8) takes the form

$$\frac{\mathscr{E}^v}{2\pi} \simeq N_z - 2h_v + 2[N_z - 1](\cos\theta_v - 1) + \ldots.$$

The energy reaches a minimum at $N_z = 1$, which corresponds to disks with an infinitely small aspect ratio.

Thus, for finite disk parameters, the transition to the saturated state takes place at a finite value of the core radius W, which is given by Eq. (10) and tends to infinity when $\varepsilon \longrightarrow 0$.

The energy of the vortex state of a disk with a radius much larger than the size of the vortex core is given by Eq. (1) with N_x being replaced by $N_v \simeq 2(l/R)^2\ln(R/W)$. In this case, the equilibrium magnetization far from the vortex core is

$$\cos\theta_v = \frac{h}{h_v}, \quad h_v = N_z - N_v. \qquad (11)$$

The saturation field h_v is plotted in Fig. 2 as a function of the disk thickness (solid line). Line 2 in Fig. 1 corresponds to a disk in which the transition to the saturated state occurs from the vortex state. In this case, the theoretical value $h_v \approx 0.305$ agrees well with the result of modeling, $h_v \approx 0.32$. Analogous calculations can also be performed for a disk that is initially in the vortex state. Figure 5 shows the results of micromagnetic modeling for a disk with $R = 50$ nm and $d = 20$ nm. The value $h_v \approx 0.61$ obtained from the numerical modeling agrees very well with an analytical estimate $h_v \approx 0.615$.

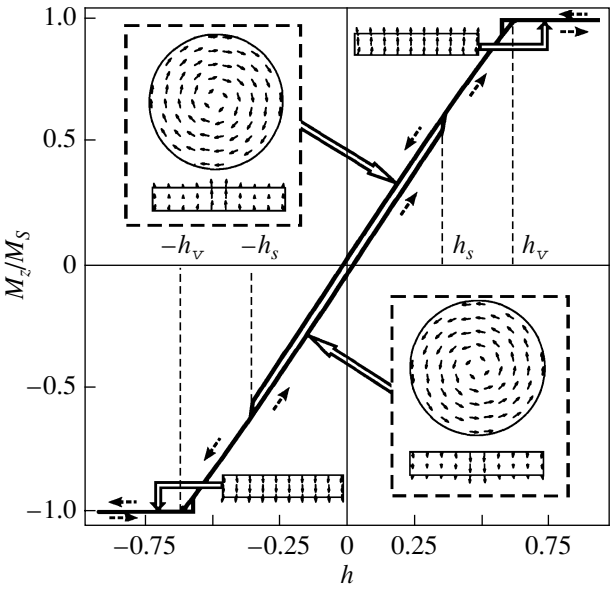

Fig. 5. Hysteresis loop obtained by micromagnetic modeling for a permalloy disk in a vortex state (the disk thickness and radius are 20 and 50 nm, respectively).

4. SWITCHING OF VORTEX POLARIZATION AND HYSTERESIS OF NANODISK

Switching of magnetization of nanodisks in the vortex state is accompanied by hysteresis. The hysteresis in this case arises because there are two types of vortices differing in the polarization direction, i.e., the direction of the magnetization in the center of the vortex [23]. In the absence of an external field, vortices of opposite polarization have the same energy. Under the influence of a magnetic field, vortices pass to a so-called cone state. The vortices polarized along the field direction (easy vortices) become energetically more favorable [5]. However, within the continuum model, the transition to hard vortices is impossible because of the continuity of the magnetization field (vortices with opposite polarizations are separated by an infinite barrier). In a real discrete system, the situation is different: the vortex polarization is not a topological invariant and the polarization switching can take place. For example, the switching can occur under a circular magnetic field [24–26].

Instability of vortices in an easy-plane magnet subjected to a dc magnetic field applied along the hard axis of the magnet was studied in [6]. The discreteness was taken into account in [6] by introducing higher spatial derivatives into the Hamiltonian. The instability of hard vortices leads to polarization switching and is accompanied by hysteresis, which was observed in the Monte Carlo numerical simulation of vortices in an easy-plane magnet performed in [7]. All of the above studies dealt with easy-plane magnets wherein the vortices were nonlinear excitations of the system. In our case of nanodisks, a vortex is the ground state of the system.

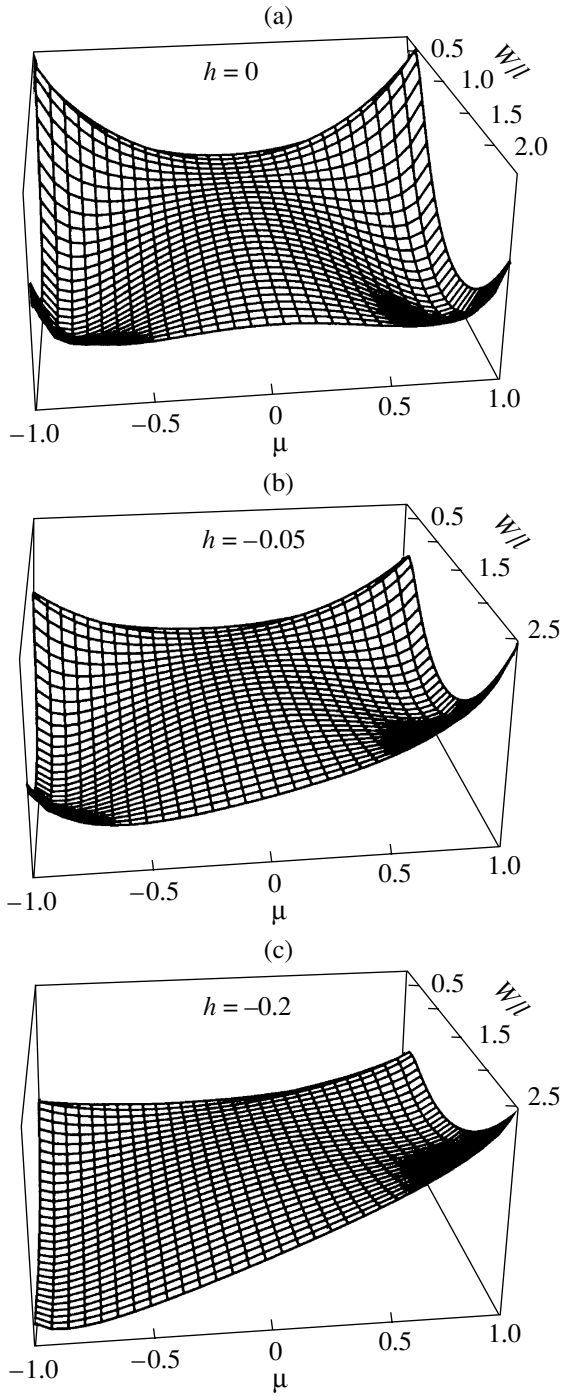

Fig. 6. Energy of the disk calculated from Eq. (12) for various values of the external field h: (a) 0, (b) –0.05, and (c) –0.2. The calculations are performed using a cutoff radius $a/l = 1/5.3$. For these parameter values, the magnetization switching occurs at $h = -0.12$.

To describe the vortex polarization switching in a nanodisk with inclusion of the magnetostatic interaction, we use ansatz (4) with the difference that the amplitude μ at the vortex center is now a variational parameter. Thus, we assume that, in the process of switching, the vortex passes through the in-plane vortex state. This assumption is valid only for sufficiently thin disks ($d \lesssim 4l$); in thicker disks, the polarization switching occurs via the formation of a Bloch point [9].

The discreteness is taken into account by introducing a cutoff radius a (which is of the order of the magnetic lattice constant) when calculating the integrals in Eq. (5). In general, the system is described by variational parameters θ_v, W, and μ. For simplicity sake, we only consider the case of very thin disks with $N_v \ll N_z = 1$. According to Eq. (11), the equilibrium magnetization of a vortex in the cone state is $\cos\theta_v \approx h$; hence, the system has only two variational parameters, W and μ. The energy of the vortex state in this case is (to within a constant)

$$\mathcal{E}^v = \frac{4\pi l^2}{R^2 - a^2}\left[(1-h^2)\ln\frac{R}{a} + \mathcal{E}\right] - 2\pi h^2,$$

$$\mathcal{E} = \int_{a/W}^{\infty} x\,dx\left\{\frac{W^2\nu^2 f^2(x)}{l^2} - \frac{\nu f(x)}{x^2}[\nu f(x) + 2h] + \frac{\nu^2 f'(x)^2}{1 - h^2 - 2h\nu f(x) - \nu^2 f^2(x)}\right\}, \quad (12)$$

$$\nu = \mu - h.$$

Here, we used the fact that the function $f(x)$ is localized, which allows one to extend the upper limit of integration to infinity.

The results of numerical calculations of the nanodisk energy $\mathcal{E}$ as a function of variational parameters μ and W are shown in Fig. 6. In the absence of a field, the energy is described by a two-well potential in which the vortices with $\mu \approx \pm 1$ are equal (Fig. 6a). The polarization μ corresponding to the minima of $\mathcal{E}$ is not exactly ±1 because of a nonzero cutoff radius a, which corresponds to the intermediate vortex state obtained in [19].

In the presence of an external field, the vortices are separated into energetically favorable (easy) and unfavorable (hard) vortices. We assume that the polarization of a vortex in a zero external magnetic field is positive. Therefore, under a negative external field, the vortices with a positive polarization become hard and the vortices with a negative polarization become easy. They are separated by a finite-height barrier (Fig. 6b). As the field increases further, the height of the barrier decreases and switching occurs at a certain critical point $|h| = h_s$ (Fig. 6c). Figure 7a shows the results of calculation of the amplitude $\mu(h)$ at the vortex center for various values of a. The field dependence of the core radius is shown in Fig. 7b. The solid lines in Fig. 7 correspond to the parameter values for permalloy; the cutoff radius is assumed to be equal to the interatomic distance in permalloy ($a = 0.3$ nm) and the exchange length is taken to be $l = 5.3$ nm. The dashed lines in Fig. 7 correspond to the parameters used in Fig. 6 ($a/l =$

1/5.3). The values of μ and W used in Fig. 7 are obtained by numerically solving the set of equations

$$\frac{\partial \mathscr{E}}{\partial \mu} = 0, \quad \frac{\partial \mathscr{E}}{\partial W} = 0. \tag{13}$$

The minimum magnitude of the external field h for which the set Eq. (13) has no solution in the range $0 < \mu < 1$ is taken to be the critical field h_s for the switching of vortex core polarization.

In order to study the dependence of the core radius on the applied field analytically, we rewrite Eq. (12) in the form

$$\mathscr{E} = 2\int_0^{e^{-\xi}} \frac{t\ln t\,dt}{\left(t-\frac{1-h}{\nu}\right)\left(t+\frac{1+h}{\nu}\right)} - h\nu E_1(\xi) - \frac{\nu^2}{2}E_1(2\xi) + \frac{W^2\nu^2}{4l^2}e^{-2\xi}, \tag{14}$$

$$\xi = \frac{a^2}{W^2}.$$

Here, $E_1(x)$ is the integral exponential function. Since the quantity a is of the order of the lattice constant and, hence, ξ is close to zero, we can use the asymptotic expression

$$\mathscr{E} \sim \text{const} + \left(h\nu + \frac{\nu^2}{2}\right)\ln\xi + \frac{\nu^2 a^2}{4l^2\xi}.$$

The value of W minimizing this energy is given by

$$W = l\sqrt{2\frac{\mu+h}{\mu-h}}. \tag{15}$$

Equation (15) is valid for an infinitely thin disk. It is seen that the vortex core radius tends to infinity when $h \longrightarrow 1$. This confirms the conclusions drawn in the previous section.

The critical field for polarization switching depends substantially on the cutoff radius a (Fig. 8). It follows from Fig. 8 that there is a certain critical value a' for which the critical field $h_s = 0$, which corresponds to the transition between out-of-plane and in-plane vortices [19]. In the calculations presented here, $a'/l = 0.3$, which coincides with the result obtained in [19] for an infinitely thin disk.

The dependence of the critical field on the cutoff radius can be closely approximated by the function

$$h_s(a) = \alpha\ln\frac{a}{a'} + \beta\ln^2\frac{a}{a'} + \gamma\left(\frac{a-a'}{a'}\right)^2, \tag{16}$$

which coincides with the results of numerical calculations with an accuracy of 6.9×10^{-3} for $\alpha = 0.09$, $\beta = 0.01$, and $\gamma = 0.64$ (Fig. 8).

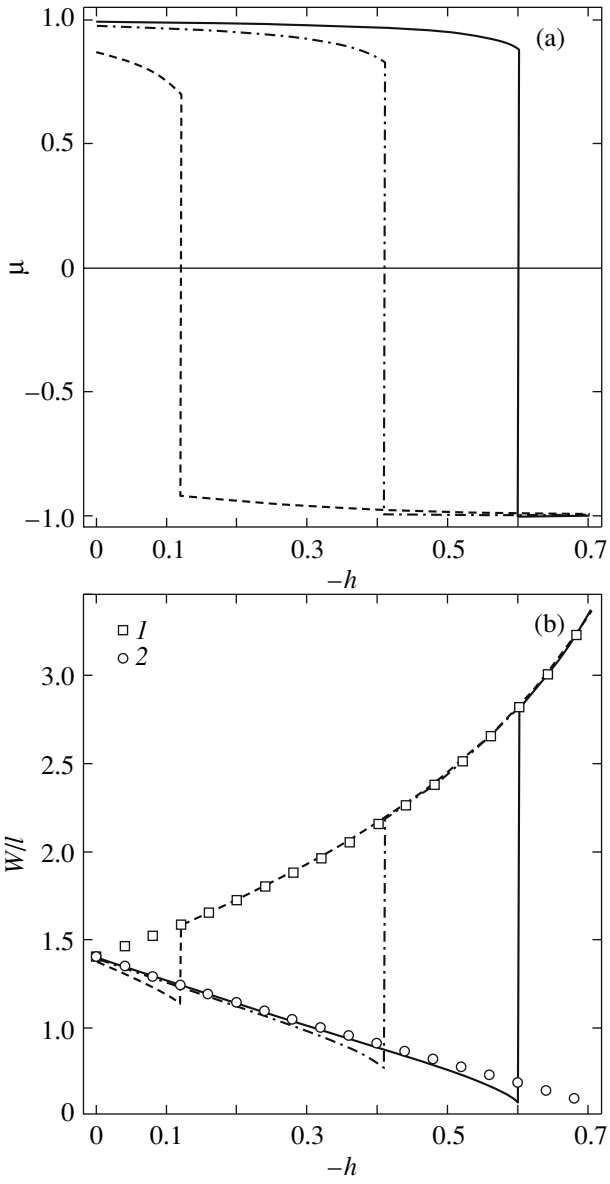

Fig. 7. (a) Vortex polarization μ and (b) vortex core radius W as functions of the applied field for various values of the cutoff radius a/l: 0.3/5.3 (solid line), 0.5/5.3 (dash-dotted line), and 1.0/5.3 (dashed line). Points *1* and *2* correspond to Eq. (15) with $\mu = 1$ for easy ($h > 0$) and hard ($h < 0$) vortices, respectively.

The theoretical calculations are in qualitative agreement with the results of micromagnetic modeling (Fig. 5), but there is a quantitative discrepancy between the modeling data ($h_s \approx 0.35$) and theoretical calculations ($h_s \approx 0.6$). This difference can be explained by the fact that, in the modeling, the role of the cutoff radius is played by the discretization step, which is severalfold larger than the corresponding interatomic distance because of limiting computational resources. The calculated hysteresis loops are in sufficiently good agreement with the experimental data from [8].

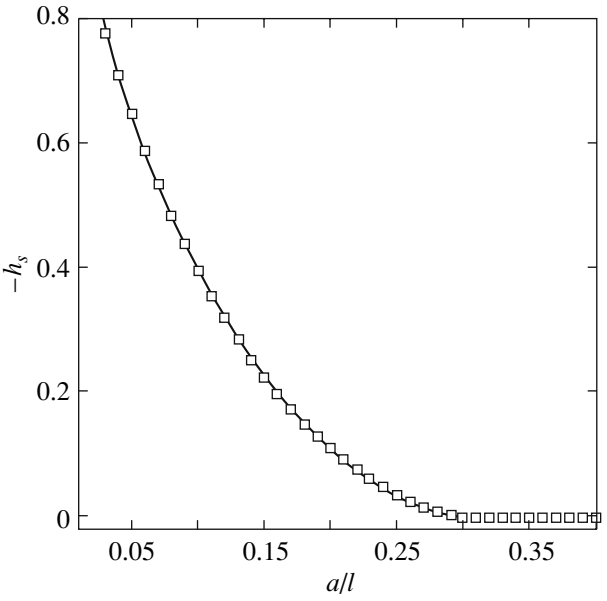

Fig. 8. Critical field for vortex polarization switching h_s as a function of the cutoff radius. Points are numerical calculations, and the solid line corresponds to the approximate equation (16).

The remanent magnetization in the hysteresis loop is due solely to the vortex core magnetization

$$M_r = \frac{M_S}{\pi R^2}\int d^2x \cos\theta(r)|_{h=0} \simeq 2M_S\frac{l^2}{R^2}.$$

Here, we took into account that $W = l\sqrt{2}$ in the absence of a magnetic field [19]. The coercive force h_c can be found from the equation $\int d^2x \cos\theta(r)|_{h=-h_c} = 0$. If we disregard the variation of the core in a small external field, we get the estimate $h_c \simeq 2l^2/R^2$.

5. CONCLUSIONS

We have studied in detail magnetization switching in magnetic nanodisks in an external field normal to the disk plane. Both single-domain nanoparticles and particles in a vortex state have been discussed. It has been shown that the process of magnetization switching in single-domain particles can be accompanied by the formation of an intermediate vortex state. The magnetic phase diagram of the disk has been constructed. It should be noted that the phase boundaries can be somewhat smeared due to the regions of instability of various phases, e.g., with respect to the displacement of the vortex center [27]. These bistability effects were observed experimentally in [28]. Moreover, intermediate states, such as the nonuniform vortex-free *C* state, can exist near the phase boundaries [29]. Investigating these effects is beyond the scope of this work.

The magnetization reversal process is accompanied by the switching of the vortex core polarization. We have suggested a simple analytical continuum model describing the switching process sufficiently well. All of the obtained theoretical results have been confirmed by micromagnetic modeling.

ACKNOWLEDGMENTS

The authors are grateful to Profs. Y.B. Gaididei and F.G. Mertens for useful discussions.

All the micromagnetic modeling data were obtained on a high-performance computing cluster at Kiev University [30]. The authors are also grateful to the University of Bayreuth, Germany, where part of this work was performed.

This work was supported by the Joint Ukraine–German project, DLR grant UKR 05/005. One of the authors (D.D.Sh.) is also grateful to the Alexander von Humboldt Foundation for financial support.

REFERENCES

1. R. Skomski, J. Phys. C: Solid State Phys. **15**, R841 (2003).
2. S. D. Bader, Rev. Mod. Phys. **78**, 1 (2006).
3. C. A. Ross, M. Hwang, M. Shima, J. Y. Cheng, M. Farhoud, T. A. Savas, H. I. Smith, W. Schwarzacher, F. M. Ross, M. Redjdal, and F. B. Humphrey, Phys. Rev. B: Condens. Matter **65**, 144417 (2002).
4. R. P. Cowburn, J. Magn. Magn. Mater. **242–245**, 505 (2002).
5. B. A. Ivanov and D. D. Sheka, Fiz. Nizk. Temp. (Kharkov) **21** (11), 1148 (1995) [Low Temp. Phys. **21** (11), 881 (1995)].
6. B. A. Ivanov and G. M. Wysin, Phys. Rev B: Condens. Matter **65**, 134434 (2002).
7. K. W. Lee and C. E. Lee, Phys. Rev. B: Condens. Matter **70**, 144420 (2004).
8. T. Okuno, K. Shigeto, T. Ono, K. Mibu, and T. Shinjo, J. Magn. Magn. Mater. **240**, 1 (2002).
9. A. Thiaville, J. M. Garcia, R. Dittrich, J. Miltat, and T. Schrefl, Phys. Rev. B: Condens. Matter **67**, 094410 (2003).
10. R. I. Joseph, J. Appl. Phys. **37**, 4639 (1966).
11. *The Object Oriented MicroMagnetic Framework* (http://math.nist.gov/oommf/).
12. K. Y. Guslienko and V. Novosad, J. Appl. Phys. **96**, 4451 (2004).
13. E. Feldtkeller and H. Thomas, Phys. Kondens. Mater. **4**, 8 (1965).
14. A. Hubert and R. Schäfer, *Magnetic Domains* (Springer, Berlin, 1998).
15. G. Gioia and R. D. James, Proc. R. Soc. London, Ser. A **453**, 213 (1997).
16. B. A. Ivanov and C. E. Zaspel, Appl. Phys. Lett. **81**, 1261 (2002).

17. D. D. Sheka, J. P. Zagorodny, J. G. Caputo, Y. Gaididei, and F. G. Mertens, Phys. Rev. B: Condens. Matter **71**, 134420 (2005).

18. J.-G. Caputo, Y. Gaididei, F. G. Mertens, and D. D. Sheka, cond-mat/0607362.

19. V. P. Kravchuk, D. D. Sheka, and Y. B. Gaididei, J. Magn. Magn. Mater. **310**, 116 (2007).

20. A. Aharoni, J. Appl. Phys. **68**, 2892 (1990).

21. K. L. Metlov and K. Y. Guslienko, J. Magn. Magn. Mater. **242–245**, 1015 (2002).

22. R. Höllinger, A. Killinger, and U. Krey, J. Magn. Magn. Mater. **261**, 178 (2003).

23. A. M. Kosevich, B. A. Ivanov, and A. S. Kovalev, *Nonlinear Waves of Magnetization: Dynamical and Topological Solitons* (Naukova Dumka, Kiev, 1983) [in Russian].

24. A. S. Kovalev and J. E. Prilepsky, Fiz. Nizk. Temp. (Kharkov) **28** (12), 1292 (2002) [Low Temp. Phys. **28** (12), 921 (2002)].

25. A. S. Kovalev and J. E. Prilepsky, Fiz. Nizk. Temp. (Kharkov) **29** (2), 71 (2003) [Low Temp. Phys. **29** (1), 55 (2003)].

26. J. P. Zagorodny, Y. Gaididei, F. G. Mertens, and A. R. Bishop, Eur. Phys. J. B **31**, 471 (2003).

27. N. Usov and S. E. Peschanyĭ, Fiz. Met. Metalloved. **78**, 13 (1994).

28. H. F. Ding, A. K. Schmid, D. Li, K. Y. Guslienko, and S. D. Bader, Phys. Rev. Lett. **94**, 157202 (2005).

29. Z.-H. Wei, M.-F. Lai, C.-R. Chang, N. Usov, J. Wu, and J.-Y. Lai, J. Magn. Magn. Mater. **282**, 11 (2004).

30. *Kyiv National Taras Shevchenko University High-Performance Computing Cluster* (http://www.unicc.kiev.ua).

Translated by G. Tsydynzhapov